

Joint Transmit and Reflective Beamforming for RIS-assisted Secret Key Generation

Lei Hu*, Guyue Li*[†], Xuewen Qian[¶], Derrick Wing Kwan Ng^{||}, and Aiqun Hu^{†‡},

*School of Cyber Science and Engineering, Southeast University, Nanjing, 210096, China

[†]Purple Mountain Laboratories for Network and Communication Security, Nanjing, 210096, China

[¶]CentraleSupélec, Paris-Saclay University, Paris, France

[‡]National Mobile Communications Research Laboratory, Southeast University, Nanjing, 210096, China

^{||}School of Electrical Engineering and Telecommunications, University of New South Wales, Sydney, NSW, 2052, Australia

Corresponding author: Guyue Li, Email: guyuilee@seu.edu.cn

Abstract—Reconfigurable intelligent surface (RIS) is a promising technique to enhance the performance of physical-layer key generation (PKG) due to its ability to smartly customize the radio environments. Existing RIS-assisted PKG methods are mainly based on the idealistic assumption of an independent and identically distributed (i.i.d.) channel model at both the transmitter and the RIS. However, the i.i.d. model is inaccurate for a typical RIS in an isotropic scattering environment. Also, neglecting the existence of channel spatial correlation would degrade the PKG performance. In this paper, we establish a general spatially correlated channel model in multi-antenna systems and propose a new PKG framework based on the transmit and the reflective beamforming at the base station (BS) and the RIS. Specifically, we derive a closed-form expression for characterizing the key generation rate (KGR) and obtain a globally optimal solution of the beamformers to maximize the KGR. Furthermore, we analyze the KGR performance difference between the one adopting the assumption of the i.i.d. model and that of the spatially correlated model. It is found that the beamforming designed for the correlated model outperforms that for the i.i.d. model while the KGR gain increases with the channel correlation. Simulation results show that compared to existing methods based on the i.i.d. fading model, our proposed method achieves about 5 dB performance gain when the BS antenna correlation ρ is 0.3 and the RIS element spacing is half of the wavelength.

I. INTRODUCTION

The inherent broadcast nature of wireless medium is vulnerable to security breaches, attracting passive or active attacks from potential eavesdroppers [1]. In contrast to conventional encryption schemes that experience difficulties in key distribution, physical-layer key generation (PKG) provides an alternative approach to establish symmetric keys between the legitimate parties. By exploiting the intrinsic randomness and the reciprocity of wireless channels, PKG is information-theoretically secure. Nevertheless, the essential premise to ensure the security of secret key in PKG is the existence of rich-scattering and dynamically varying channels. Unfortunately, this condition can hardly be satisfied to guarantee key generation performance in some harsh propagation scenarios, such as static and shadowed environments. As a result, there is a need for new technologies to improve PKG performance.

Recently, the emergence of reconfigurable intelligent surface (RIS) provides a promising means to address the afore-

mentioned problems. RIS is a programmable and reconfigurable metasurface consisting of a large number of passive elements, which can be controlled collaboratively to alter the signal propagation environment. Since the key generation performance relies on the properties of fading channels, RIS could be the key enabler for improving the PKG. Inspired by this, there are several studies on the design of RIS-assisted PKG systems. For example, in static environments, a RIS-induced randomness method was proposed in [2] and the experiments in [3] demonstrated its effectiveness. In addition, the authors of [1], [4], [5] investigated the optimization of RIS beamforming in dynamic environments to further improve the key generation rate (KGR). Nevertheless, all of these works are based on the independent and identically distributed (i.i.d.) Rayleigh fading model for the RIS-related channels. In practice, the non-negligible spatial correlations exist among RIS elements due to their sub-wavelength sizes. More importantly, these correlations may jeopardize the PKG performance if they are not taken into account in the system design [6]. In addition, only a single-antenna BS was considered in these works, e.g., [1]–[5] and their results are not applicable to the case of multi-antenna. Indeed, the RIS-assisted PKG methods in multi-antenna spatially correlated channels are still unknown.

To fill this gap, this paper investigates a RIS-assisted PKG method in a multi-antenna system with the consideration of the spatial correlation between the BS and the RIS. The main contributions of this paper are listed as follows:

- We propose a novel transmit and reflective beamforming based RIS-assisted PKG framework in spatially correlated channels. We formulate the design of beamforming as an optimization problem by deriving the closed-form KGR expression.
- We design the globally optimal transmit and reflective beamforming vector by decomposing the optimization problem into two sub-problems and optimizing them separately. Also, our analysis shows that the optimal beamforming outperforms existing designs adopting the i.i.d. channel assumption.
- Simulation results show that compared with existing

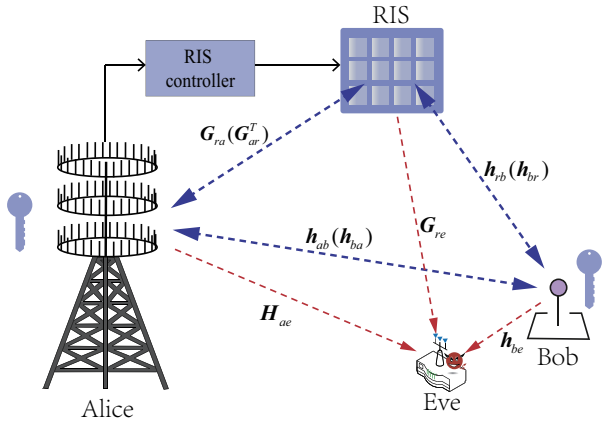


Fig. 1. The model of RIS-assisted PKG based on transmit and reflective beamforming.

methods that ignore the spatial correlation, the optimal design achieves about 5 dB gain when the antenna correlation coefficient is 0.3 and the element spacing is half of the wavelength. Moreover, the KGR gain increases with the spatial correlation at both the BS and the RIS.

II. SYSTEM MODEL

As shown in Fig. 1, we study a RIS-assisted key generation method in a multiple-input single-output multi-antenna eavesdropper (MISOME) system, in which a multi-antenna base station (BS), Alice, and a single-antenna user, Bob, aim to generate symmetric keys [4], [5] from the wireless channel with the help of a RIS adopting the time-division duplexing (TDD) protocol. Meanwhile, a multi-antenna eavesdropper, Eve, intends to obtain the key information from her received signals. We assume that Alice and Eve are equipped with M and K antennas, respectively. The RIS consists of N passive reflecting elements and introduces phase shifts to the impinging signals to facilitate key generation. Since the spatial correlation affects the secret key rate, we consider the general spatial correlation channel model at both the RIS and the BS.

A. Channel Model

The direct channels of Alice-to-Bob, Eve-to-Bob, and Alice-to-Eve are denoted by $\mathbf{h}_{ab} \in \mathbb{C}^{M \times 1}$, $\mathbf{h}_{eb} \in \mathbb{C}^{K \times 1}$, and $\mathbf{H}_{ae} \in \mathbb{C}^{K \times M}$, respectively, where $\mathbb{C}^{A \times B}$ denotes the space of complex matrices of size $A \times B$. $\mathbf{h}_{ak} \in \mathbb{C}^{M \times 1}$ denotes the channel from Alice to Eve's k -th antenna, $k \in \{1, \dots, K\}$. When a RIS is involved in the PKG system, it introduces additional channels. Specifically, the channels of RIS-to-Alice, RIS-to-Bob, and RIS-to-Eve are represented as $\mathbf{G}_{ra} \in \mathbb{C}^{M \times N}$, $\mathbf{h}_{rb} \in \mathbb{C}^{N \times 1}$, and $\mathbf{G}_{re} \in \mathbb{C}^{K \times N}$, respectively. $\mathbf{h}_{rk} \in \mathbb{C}^{M \times 1}$ denotes the channel from the RIS to Eve's k -th antenna. To account for the spatial correlation, the

channel matrices are described by employing the Kronecker correlation channel model as

$$\mathbf{G}_{ra} = \mathbf{G}_{ar}^T = \beta_{ar}^{\frac{1}{2}} \mathbf{R}_S^{\frac{1}{2}} \tilde{\mathbf{H}} \mathbf{R}_I^{\frac{1}{2}}, \quad (1)$$

$$\mathbf{h}_{ri} = \mathbf{h}_{ir} = \beta_{ir}^{\frac{1}{2}} \mathbf{R}_I^{\frac{1}{2}} \tilde{\mathbf{h}}_{ir}, \quad i \in \{b, k\}, \quad (2)$$

$$\mathbf{h}_{aj} = \mathbf{h}_{ja} = \beta_{ja}^{\frac{1}{2}} \mathbf{R}_S^{\frac{1}{2}} \tilde{\mathbf{h}}_{ja}, \quad j \in \{b, k\}, \quad (3)$$

respectively, where $\mathbf{R}_S \in \mathbb{C}^{M \times M}$ and $\mathbf{R}_I \in \mathbb{R}^{N \times N}$ are the spatial correlation matrices at Alice and the RIS, respectively [6]. The elements $[\mathbf{R}_S]_{m,n}$ and $[\mathbf{R}_I]_{m,n}$ represent the correlation between the m -th antenna/element and the n -th antenna/element. In addition, $\tilde{\mathbf{H}} \in \mathbb{C}^{M \times N}$, $\tilde{\mathbf{h}}_{ir} \in \mathbb{C}^{N \times 1}$, and $\tilde{\mathbf{h}}_{ja} \in \mathbb{C}^{M \times 1}$ are random matrices with i.i.d. Gaussian random entries of zero mean and unit variance. β_{ar} , β_{ir} , and β_{ja} are the path loss of the corresponding channels, respectively.

B. PKG Framework Based on Transmit and Reflective Beamforming

Now, we propose a new framework to take full advantages of the RIS-assisted PKG in multi-antenna systems. In PKG, Alice and Bob first perform channel probing to acquire the reciprocal channel estimation. The process of channel probing is described as follows.

Step 1: Uplink channel sounding. Bob transmits the publicly known pilot $s_u \in \mathbb{C}$ with $s_u^* s_u = 1$. Then, the equivalent baseband signal received at Alice and Eve are expressed as

$$\mathbf{y}_l^u = \sqrt{P_B} (\mathbf{G}_{rl} \Phi \mathbf{h}_{br} + \mathbf{h}_{bl}) s_u + \mathbf{z}_l, \quad l \in \{a, e\}, \quad (4)$$

respectively, where $\Phi = \text{diag}\{\mathbf{v}\}$ with each element $|v_n| = 1, \forall n \in \{1, \dots, N\}$, is the reflection coefficients matrix of the RIS. $\text{diag}(\mathbf{x})$ and $|x|$ denotes a diagonal matrix and the modulus of a complex scalar, respectively. In addition, P_B is the transmit power of Bob. The noise follows the circularly symmetric complex Gaussian distribution, i.e., $\mathbf{z}_a \sim \mathcal{CN}(0, \sigma_a^2 \mathbf{I}_{M \times M})$, $\mathbf{z}_e \sim \mathcal{CN}(0, \sigma_e^2 \mathbf{I}_{K \times K})$, where σ_a^2 and σ_e^2 are the noise variances of Alice and Eve, respectively. Then, Alice and Eve perform the least square (LS) estimation¹ as

$$\hat{\mathbf{h}}_l^u \triangleq s_u^* \mathbf{y}_l^u = \sqrt{P_B} (\mathbf{G}_{rl} \Phi \mathbf{h}_{br} + \mathbf{h}_{bl}) + \tilde{\mathbf{z}}_l^u, \quad l \in \{a, e\}, \quad (5)$$

respectively, where the estimation noise is $\tilde{\mathbf{z}}_l^u = s_u^* \mathbf{z}_l^u$.

Step 2: Downlink channel sounding. Alice sends the pilot $s_d \in \mathbb{C}$ with $s_d^* s_d = 1$, and the signals received at Bob and Eve are

$$\mathbf{y}_b^d = (\mathbf{h}_{rb}^T \Phi \mathbf{G}_{ar} + \mathbf{h}_{ab}^T) \mathbf{w} s_d + \mathbf{z}_b^d, \quad (6)$$

$$\mathbf{y}_e^d = (\mathbf{G}_{re} \Phi \mathbf{G}_{ar} + \mathbf{H}_{ae}) \mathbf{w} s_d + \mathbf{z}_e^d, \quad (7)$$

respectively, where \mathbf{w} is the transmit beamforming vector at Alice that satisfies $\|\mathbf{w}\|^2 \leq P_A$. $\|\cdot\|$ denotes the Euclidean norm. \mathbf{z}_b^d and \mathbf{z}_e^d are the additive Gaussian noise with $\mathbf{z}_b^d \sim \mathcal{CN}(0, \sigma_b^2)$ and $\mathbf{z}_e^d \sim \mathcal{CN}(0, \sigma_e^2 \mathbf{I}_{K \times K})$. After the LS estimation, Bob and Eve obtain the channel estimates as

$$\hat{\mathbf{h}}_b \triangleq s_d^* \mathbf{y}_b^d = (\mathbf{h}_{rb}^T \Phi \mathbf{G}_{ar} + \mathbf{h}_{ab}^T) \mathbf{w} + \tilde{\mathbf{z}}_b, \quad (8)$$

$$\hat{\mathbf{h}}_e \triangleq s_d^* \mathbf{y}_e^d = (\mathbf{G}_{re} \Phi \mathbf{G}_{ar} + \mathbf{H}_{ae}) \mathbf{w} + \tilde{\mathbf{z}}_e^u, \quad (9)$$

¹The LS is adopted since it has been widely used in practical systems [1].

respectively, where the noises are $\tilde{z}_b^d = s_d^* z_b^d$ and $\tilde{z}_e^u = s_d^* z_e^u$, respectively.

Step 3: Reciprocal components acquisition. Since the estimations obtained by Alice and Bob, as shown in (5) and (8), are quite different, we multiply Alice's channel estimation \hat{h}_a^u by \mathbf{w} to obtain the combined reciprocal channel gain as

$$\hat{h}_a \triangleq \mathbf{w}^T \hat{h}_a^u = \sqrt{P_B} \mathbf{w}^T (\mathbf{G}_{ra} \Phi \mathbf{h}_{br} + \mathbf{h}_{ba}) + z_a, \quad (10)$$

where the noise is $z_a = \mathbf{w}^T \tilde{z}_a^u$.

Consequently, Alice's combined channel gain, \hat{h}_a , and Bob's channel gains, \hat{h}_b , are highly correlated. After the following procedures of the PKG, i.e., quantization, information reconciliation, and privacy amplification, the channel gains are finally converted into secret keys [7]. Since these steps are similar to those used in existing PKG methods, in this paper, we focus on the channel probing step, where the transmit and reflective beamforming are optimized to maximize the KGR.

III. PROBLEM FORMULATION

In this section, we formulate an optimization problem to find the optimal transmit beamforming \mathbf{w} and the reflective beamforming \mathbf{v} by deriving the closed-form KGR expression.

First, the secret key rate is defined as the conditional mutual information of legitimate parties' channel estimations given the observation of Eve [1], which is expressed as

$$R_{\text{SK}} \triangleq \mathcal{I}(\hat{h}_a; \hat{h}_b | \hat{h}_e^u, \hat{h}_e^d), \quad (11)$$

where $\mathcal{I}(X; Y)$ is the mutual information of random variables X and Y . In this paper, we assume that Eve is located at least half-wavelength away from Alice and Bob. Hence, the eavesdropping channels are independent of the legitimate channels². In this case, the KGR is given by [1]

$$R_{\text{SK}} = \mathcal{I}(\hat{h}_a; \hat{h}_b) = \log_2 \frac{\mathcal{R}_{a,a} \mathcal{R}_{b,b}}{\det(\mathbf{R}_{ab})}, \quad (12)$$

where $\mathcal{R}_{i,j} = \mathbb{E}\{\hat{h}_i \hat{h}_j^H\}$, $i, j \in \{a, b\}$, $\det(\cdot)$ is the matrix determinant, $\mathbb{E}\{\cdot\}$ denotes the statistical expectation, and

$$\mathbf{R}_{ab} = \begin{bmatrix} \mathcal{R}_{a,a} & \mathcal{R}_{a,b} \\ \mathcal{R}_{b,a} & \mathcal{R}_{b,b} \end{bmatrix}. \quad (13)$$

Substituting the channel estimations into (12) and assuming $\sigma_a^2 = \sigma_b^2 = \sigma^2$ for simplicity, R_{SK} is expressed as (14) at the top of the next page, where $\tilde{\mathbf{R}}_I = \mathbf{R}_I^T \circ \mathbf{R}_I$, $\beta_r = \beta_{ar} \beta_{br}$, and \circ denotes Hadamard product.

Proof: See Appendix A. ■

Thus, the beamforming design can be formulated as

$$\mathcal{P} : \underset{\mathbf{w}, \mathbf{v}}{\text{maximize}} \quad R_{\text{SK}} \quad (15)$$

$$\text{subject to } |v_n| = 1, \forall n \in \{1, \dots, N\}, \quad (15a)$$

$$\|\mathbf{w}\|^2 \leq P_A, \quad (15b)$$

where (15a) represents the unit modulus constraint of each reflection coefficient, while (15b) indicates the transmit beamforming is constrained by the maximum transmit power.

²Due to the space limitation, the case where Eve experiences a correlated channel will be investigated in the extended journal version.

IV. PROPOSED SOLUTION TO PROBLEM \mathcal{P}

In this section, we jointly optimize the transmit beamforming \mathbf{w} and the reflective beamforming \mathbf{v} to maximize the KGR. To tackle the non-convex problem in (15), we decompose the problem into two sub-problems and optimize them to obtain the globally optimal solution.

A. Problem Decomposition

It could be found that in problem \mathcal{P} , the objective function (14) contains high-order terms in \mathbf{w} and \mathbf{v} , while the unit modulus constraint (15a) and quadratic equality constraints (15b) are both non-convex and the optimization variables are coupled. To tackle this problem, we first decompose the problem into two sub-problems with respect to \mathbf{w} and \mathbf{v} , respectively, using the following Lemma.

Lemma 1. *The objective function in \mathcal{P} increases monotonically with $\mathbf{w}^T \mathbf{R}_S \mathbf{w}^*$ ($\beta_r \mathbf{v}^H \tilde{\mathbf{R}}_I \mathbf{v} + \beta_{ba}$).*

Proof: See Appendix B. ■

Since $\mathbf{w}^T \mathbf{R}_S \mathbf{w}^*$ and $(\beta_r \mathbf{v}^H \tilde{\mathbf{R}}_I \mathbf{v} + \beta_{ba})$ are both positive, solving problem \mathcal{P} is equivalent to maximize these two terms separately.

B. Transmit Beamforming Optimization

One of the sub-problems is to optimize the transmit beamforming vector, which is expressed as \mathcal{P}_1 by denoting $\bar{\mathbf{w}} = \mathbf{w}^*$:

$$\mathcal{P}_1 : \underset{\bar{\mathbf{w}}}{\text{maximize}} \quad \bar{\mathbf{w}}^H \mathbf{R}_S \bar{\mathbf{w}} \quad (16)$$

$$\text{subject to } \|\bar{\mathbf{w}}\|^2 \leq P_A. \quad (16a)$$

By using the Rayleigh quotient, the optimal solution to \mathcal{P}_1 is

$$\bar{\mathbf{w}}_{\text{opt}} = \sqrt{P_A} \mathbf{u}_{\lambda_{\max}}, \quad (17)$$

where $\mathbf{u}_{\lambda_{\max}}$ is the dominant eigenvector of the matrix \mathbf{R}_S corresponding to its maximum eigenvalue λ_{\max} .

C. Reflective Beamforming Optimization

After deriving the optimal transmit beamforming vector, we aim to optimize the reflection coefficients at RIS. With Lemma 1, the problem of optimizing \mathbf{v} is equivalent to

$$\mathcal{P}_2 : \underset{\mathbf{v}}{\text{maximize}} \quad \mathbf{v}^H \tilde{\mathbf{R}}_I \mathbf{v} \quad (18)$$

$$\text{subject to } |v_n| = 1, \forall n \in \{1, \dots, N\}. \quad (18a)$$

It is noted that the unit modulus constraints in (18a) are intrinsically non-convex [1]. Therefore, it is challenging to solve this problem. Nevertheless, we note that each element in $\tilde{\mathbf{R}}_I = \mathbf{R}_I^T \circ \mathbf{R}_I$ is a positive number since the covariance matrix \mathbf{R}_I is real symmetric. Based on this observation, the optimal solution is given as follows.

Theorem 2. *The optimal solution to problem \mathcal{P}_2 is the case where all elements of \mathbf{v} adopt the same phase, i.e.,*

$$\theta_n = \theta, \forall n \in \{1, \dots, N\}, \quad (19)$$

where θ could take on any value in interval $[0, 2\pi)$.

$$R_{\text{SK}} = \log_2 \frac{(P_B \mathbf{w}^T \mathbf{R}_S \mathbf{w}^* (\beta_r \mathbf{v}^H \tilde{\mathbf{R}}_I \mathbf{v} + \beta_{ba}) + \|\mathbf{w}\|^2 \sigma^2) (\mathbf{w}^T \mathbf{R}_S \mathbf{w}^* (\beta_r \mathbf{v}^H \tilde{\mathbf{R}}_I \mathbf{v} + \beta_{ba}) + \sigma^2)}{(\|\mathbf{w}\|^2 + P_B) \sigma^2 \mathbf{w}^T \mathbf{R}_S \mathbf{w}^* (\beta_r \mathbf{v}^H \tilde{\mathbf{R}}_I \mathbf{v} + \beta_{ba}) + \|\mathbf{w}\|^2 \sigma^4}. \quad (14)$$

Proof: The objective function (18) could be calculated as

$$\begin{aligned} \mathbf{v}^H \tilde{\mathbf{R}}_I \mathbf{v} &= \sum_{n=1}^N [\tilde{\mathbf{R}}_I]_{n,n} + \sum_{j=1}^N \sum_{i=1}^N [\tilde{\mathbf{R}}_I]_{i,j} v_i v_j^* \\ &= \sum_{n=1}^N [\tilde{\mathbf{R}}_I]_{n,n} + \sum_{j=1}^N \sum_{i=1, i>j}^N 2[\tilde{\mathbf{R}}_I]_{i,j} \cos(\theta_i - \theta_j). \end{aligned} \quad (20)$$

Since $\cos(\theta_i - \theta_j) \leq 1$, the maximum value could be obtained when $\theta_i = \theta_j$, $\forall i, j$. This completes the proof. \blacksquare

In the case of optimal \mathbf{w} and \mathbf{v} , the KGR only depends on the large-scale path loss, indicating the maximum KGR is dependent on the distance between Alice, Bob, and the RIS. Moreover, in the spatially correlated channel model, the optimal beamforming are determined by the spatial correlation matrices at the BS and the RIS, which could be obtained effectively by existing methods, such as [6] and [8].

V. IMPACT OF DIFFERENT BEAMFORMING METHODS ON PKG PERFORMANCE

In this section, we aim to compare the PKG performance under the assumptions of the i.i.d. channel model and the spatially correlated channel model.

A. KGR under Different Assumptions of Channel Model at BS

As shown in Lemma 1, the KGR is proportional to $\mathbf{w}^T \mathbf{R}_S \mathbf{w}^*$. Under the assumption of the i.i.d. model, the spatial correlation matrix \mathbf{R}_S is considered as an identity matrix. In this case, the design of transmit beamforming is independent of KGR. As such, random beamforming $\tilde{\mathbf{w}} = \sqrt{P_A} \tilde{\mathbf{w}}_0 / \|\tilde{\mathbf{w}}_0\|$ is applied without loss of generality, where the entries in $\tilde{\mathbf{w}}_0$ are i.i.d. random variables with zero mean. Then, the expectation of the objective function in \mathcal{P}_1 is calculated as $\mathbb{E}\{\tilde{\mathbf{w}}^T \mathbf{R}_S \tilde{\mathbf{w}}^*\} = P_A$, which is independent of the antenna number and the spatial correlation at the BS.

To investigate the performance loss caused by the design based on the i.i.d. channel assumption, we focus on a typical implementation model of multiple antennas for massive multiple-input multiple-output (MIMO). We consider a general uniform planar array (UPA) model, where the spatial correlation matrix can be approximated as $\mathbf{R}_S \approx \mathbf{R}_h \otimes \mathbf{R}_v$ [9], where \mathbf{R}_h and \mathbf{R}_v are the covariance matrices of the horizontal and the vertical uniform linear array (ULA), respectively. The ULA spatial correlation is modeled as a Toeplitz matrix with each element $[\mathbf{R}_l]_{i,j} = \rho^{|i-j|}$, $l \in \{h, v\}$, where ρ is the correlation index among the antennas. Given the optimal transmit beamforming (17), we have the following lemma.

Lemma 3. *For a UPA model, the upper and lower bounds for the $\mathbf{w}_{\text{opt}}^T \mathbf{R}_S \mathbf{w}_{\text{opt}}^*$ are given by*

$$f_l(N_H^t, N_V^t, \rho) \leq \mathbf{w}_{\text{opt}}^T \mathbf{R}_S \mathbf{w}_{\text{opt}}^* \leq f_u(N_H^t, N_V^t, \rho), \quad (21)$$

where $f_l(N_H^t, N_V^t, \rho) = P_A \frac{(N_H^t(1-\rho^2) - 2\rho(1-\rho^{N_H^t}))}{N_H^t N_V^t (1-\rho^4)} \times (N_V^t(1-\rho^2) - 2\rho(1-\rho^{N_V^t}))$ and $f_u(N_H^t, N_V^t, \rho) = P_A \frac{(1+\rho^2)(1-\rho^{N_H^t-1})(1-\rho^{N_V^t-1})}{(1-\rho)^2}$. N_H^t and N_V^t are the number of antennas at horizontal and vertical domains, respectively.

Proof: See Appendix C \blacksquare

This lemma shows that the both the upper and lower bounds increase monotonically with the correlation coefficients ρ , the number of antennas N_H^t , and N_V^t . This is because the SNR of the combined channel gain increases with the spatial correlation. Specifically, when $\rho = 0$, the bounds are $f_l(N_H^t, N_V^t, 0) = f_u(N_H^t, N_V^t, 0) = 1$, which means the optimal transmit beamforming and random beamforming achieve the same PKG performance in the i.i.d. fading channels. In addition, it can be observed that both the upper and lower bounds converge to $P_A (\frac{1+\rho}{1-\rho})^2$ as $N_H^t \rightarrow \infty$ and $N_V^t \rightarrow \infty$. This means when the BS is equipped with a large amount of antennas, the KGR depends only on the correlations among the antennas of the BS for a given power. Also, the KGR increases monotonically with the correlation coefficient ρ .

B. KGR under Different Assumptions of Channel Model at RIS

In Lemma 1, the KGR is proportional to $\mathbf{v}^H \tilde{\mathbf{R}}_I \mathbf{v}$. Under the assumption of the i.i.d. channel model adopting in existing works, the spatial correlation matrix is $\tilde{\mathbf{R}}_I = \mathbf{I}$. By employing the random reflection, the expectation of the objective function of \mathcal{P}_2 is $\mathbb{E}\{\tilde{\mathbf{v}}^H \tilde{\mathbf{R}}_I \tilde{\mathbf{v}}\} = N$, where each phase in $\tilde{\mathbf{v}}$ can be drawn from the uniform distribution, i.e., $\theta_i \sim U[0, 2\pi)$, $i \in \{1, \dots, N\}$.

Taking the spatial correlation model into account, the maximum value of $\mathbf{v}^H \tilde{\mathbf{R}}_I \mathbf{v}$ is $\|\mathbf{R}_I\|_F^2$, where $\|\cdot\|_F^2$ denotes the Frobenius norm. To characterize the impact of spatial correlation on RIS, we have the following lemma.

Lemma 4. *(Proposition 1 in [6]) In isotropic scattering environments, the spatial correlation of RIS is expressed as*

$$[\mathbf{R}_I]_{n,m} = \text{sinc} \frac{2\|\mathbf{u}_n - \mathbf{u}_m\|}{\lambda}, \quad \forall n, m \in \{1, \dots, N\}, \quad (22)$$

where $\|\mathbf{u}_n - \mathbf{u}_m\|$ denotes the distance between n -th RIS element and m -th RIS element, λ is the wavelength.

Since the sinc function $\text{sinc}(x) = \text{sinc}(\pi x) / (\pi x)$ is monotonically decreasing in interval $[0, 1)$, the entries in \mathbf{R}_I is larger as the inter-element spacing becomes smaller, when the elements distance fulfill $\|\mathbf{u}_n - \mathbf{u}_m\| \leq \frac{\lambda}{2}$. Moreover, the optimal value of $\mathbf{v}^H \tilde{\mathbf{R}}_I \mathbf{v}$ satisfies $\|\mathbf{R}_I\|_F^2 > N$ because the correlation between the elements always exists in practical RIS systems [6]. Hence, the KGR performance of the proposed reflective beamforming is better than the counterpart adopting the assumption of the i.i.d. channel model.

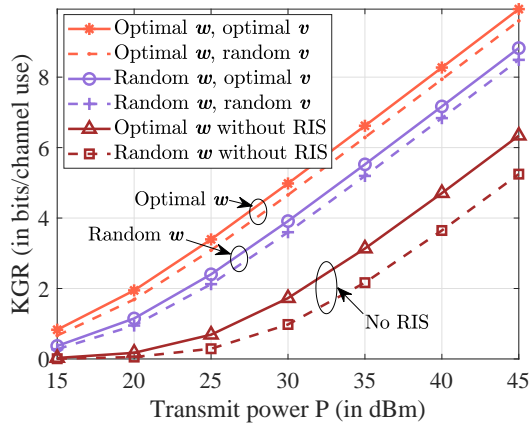


Fig. 2. The KGR achieved by different beamforming settings when $M = 16$, $\rho = 0.3$, $N = 64$, and RIS element spacing is $\lambda/2$.

VI. SIMULATION RESULTS

In this section, we evaluate the performance of the proposed method with the aid of numerical simulations. We assume that Alice, Bob, and RIS are located at $(0 \text{ m}, 0 \text{ m})$, $(70 \text{ m}, 0 \text{ m})$, and $(50 \text{ m}, 10 \text{ m})$, respectively³ [10]. Alice is equipped with a UPA antenna. The RIS is a uniform rectangular array (URA) with N_H^r elements per row and N_V^r elements per column. The large-scale path loss $\beta_{ba} = \sqrt{\zeta_0 d_{ba}^{-\alpha_{ba}}}$, where d_{ba} , ζ_0 , and α_{ba} are the distance, path loss at 1 m, and the path loss exponent, respectively. The transmit power are $P_A = P_B = P$ [1], [2], and the simulation settings are $\alpha_{ba} = 4$, $\alpha_{br} = \alpha_{ar} = 2$, $\zeta_0 = -30 \text{ dB}$, and $\sigma^2 = -80 \text{ dBm}$ [10].

A. Optimality of the Proposed Method

In Fig. 2, the KGR versus the transmit power, P , is plotted for different transmit and reflective beamforming settings. First, we observe that the KGR at all settings increases with the transmit power, since the negative impacts of noises are reduced. For comparison, the benchmarks are random beamforming based on the i.i.d. channel model and the case without RIS. It is noted that the proposed optimal design outperforms these benchmarks. Specifically, when $P \geq 20 \text{ dBm}$, the optimal setting achieves about 5 dB and 11 dB transmit power gain compared to the beamforming scheme under the i.i.d. channel assumption and the optimal transmit beamforming without RIS, respectively. This is because when correlations exist between the BS antennas and the RIS elements, the i.i.d. model fails in capturing this characteristic which degrades the KGR performance. In contrast, the proposed scheme can effectively exploit the properties of the channels to perform precise beamforming. Finally, the KGR gain of optimizing w is larger than that of optimizing v . Indeed, optimizing w is more effective than that of v in combating the noises in R_{SK} , and this aligns with the analysis in (14).

³Since the eavesdropping channels are independent of the legitimate channels in this paper, the exact location of Eve and the number of Eve's antennas has no impact on the KGR.

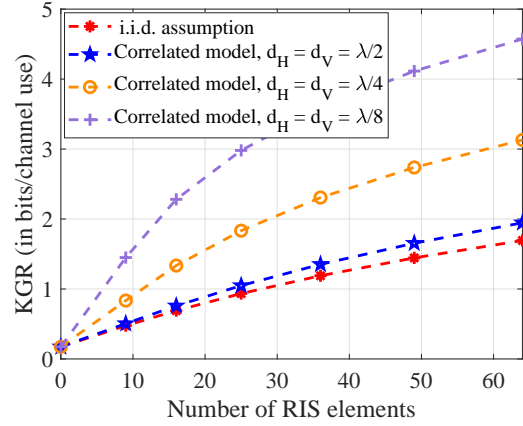


Fig. 3. The KGR achieved for different N with $N_H^r = N_V^r$, when $P = 20 \text{ dBm}$, $M = 16$, and $\rho = 0.3$.

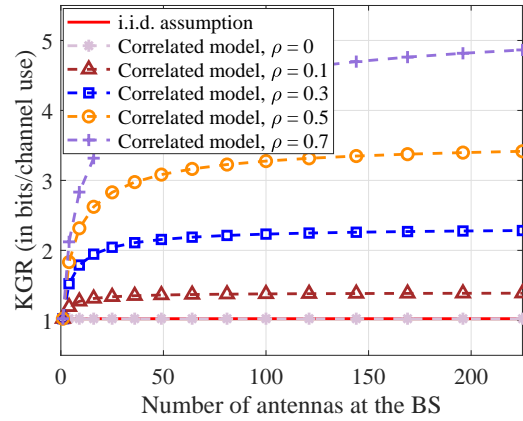


Fig. 4. The KGR versus the number of antennas M with $N_H^t = N_V^t$, when $N = 64$, $P = 20 \text{ dBm}$, and RIS element spacing is $\lambda/2$.

B. The Impact of RIS Elements Number and Size

Fig. 3 shows the KGR of different spatial correlations at RIS versus the number of RIS elements N . It is observed that the KGR of all of these cases increases with the number of RIS elements. As more elements are placed, more electromagnetic signals are reflected by the RIS to realize better KGR performance. Moreover, we notice that with the elements spacing becomes smaller, the KGR increases significantly. This is because with smaller elements spacing, the values of the spatial correlation matrix \mathbf{R}_I are larger, contributing to a higher KGR. Also, it is found that even with $\lambda/2$ RIS element spacing, the KGR of the proposed method is still slightly superior than that adopting the i.i.d. assumption. In fact, the correlation among the RIS elements is weak in $\lambda/2$ spacing, although it always exists if $N_H^r > 1$ and $N_V^r > 1$, which can be exploited by the proposed method.

C. The Impact of BS Antennas Number and Correlation

Fig. 4 shows the KGR versus the number of the antennas at the BS. As can be observed, the KGR of the design method

based on the i.i.d. fading model is identical to that of the proposed design when $\rho = 0$, which is independent of antenna number at the BS. For the cases of $\rho > 0$, the proposed method can achieve higher KGR gain, since the upper and lower bounds of the KGR both increase with the spatial correlation between antennas. Moreover, with the number of antennas increases, the KGR increases with diminishing returns. This is due to the channel hardening and the limited transmit power at the BS.

VII. CONCLUSION

In this paper, we introduced a novel transmit and passive beamforming based RIS-assisted PKG method in multi-antennas spatially correlated channels. We formulated the optimization problem and obtained a globally optimal solution to maximize the KGR. We compared the KGR performance under the assumptions of the i.i.d. channel model and the spatially correlated channel model. We found that in spatially correlated channels, the proposed beamforming design achieves higher PKG than that under the i.i.d. channel model assumption. Simulation results confirmed the performance of the proposed method and the analysis of the spatial correlation.

APPENDIX A COVARIANCE CALCULATION

First, we calculate the covariance of channel \hat{h}_a as

$$\mathcal{R}_{a,a} = P_B \mathbf{w}^T \mathbb{E} \{ \mathbf{G}_{ra} \Phi \mathbf{h}_{br} \mathbf{h}_{br}^H \Phi^H \mathbf{G}_{ra}^H \} \mathbf{w}^* + P_B \mathbf{w}^T \mathbb{E} \{ \mathbf{h}_{ba} \mathbf{h}_{ba}^H \} \mathbf{w}^* + \|\mathbf{w}\|^2 \sigma_a^2. \quad (23)$$

Assuming the BS has obtained the \mathbf{R}_S by employing [8], we can calculate the first term in (23) as

$$\mathbb{E} \{ \mathbf{G}_{ra} \Phi \mathbf{h}_{br} \mathbf{h}_{br}^H \Phi^H \mathbf{G}_{ra}^H \} \quad (24)$$

$$= \beta_r \mathbf{R}_S \mathbb{E} \{ \text{vec} \{ \tilde{\mathbf{h}}_{br}^H \mathbf{R}_I^{\frac{1}{2}} \Phi^H \mathbf{R}_I^{\frac{1}{2}} \}^H \text{vec} \{ \tilde{\mathbf{h}}_{br}^H \mathbf{R}_I^{\frac{1}{2}} \Phi^H \mathbf{R}_I^{\frac{1}{2}} \} \} \quad (25)$$

$$= \beta_r \mathbf{R}_S \mathbb{E} \{ \mathbf{v}^H ((\mathbf{R}_I^{\frac{1}{2}})^T \odot (\mathbf{R}_I^{\frac{1}{2}}))^H (\tilde{\mathbf{h}}_{br}^* \otimes \mathbf{I}_N) \times (\tilde{\mathbf{h}}_{br}^T \otimes \mathbf{I}_N) ((\mathbf{R}_I^{\frac{1}{2}})^T \odot (\mathbf{R}_I^{\frac{1}{2}})) \mathbf{v} \} \quad (26)$$

$$= \beta_r \mathbf{R}_S \mathbf{v}^H ((\mathbf{R}_I^{\frac{1}{2}})^T \odot (\mathbf{R}_I^{\frac{1}{2}}))^H ((\mathbf{R}_I^{\frac{1}{2}})^T \odot (\mathbf{R}_I^{\frac{1}{2}})) \mathbf{v} \quad (27)$$

$$= \beta_r \mathbf{R}_S \mathbf{v}^H (\mathbf{R}_I^T \circ \mathbf{R}_I) \mathbf{v}, \quad (28)$$

where \otimes and \odot denote the Kronecker product and Khatri-Rao product, respectively, $\text{vec}(\mathbf{X})$ denotes the vectorization of a matrix, and \circ denotes Hadamard product. Then, the second term in (23) is calculated as $\mathbb{E} \{ \mathbf{h}_{ba} \mathbf{h}_{ba}^H \} = \beta_{ba} \mathbf{R}_S$. Other covariances can be calculated similarly and are omitted here.

APPENDIX B PROOF OF LEMMA 1

We first denote $\mathbf{w} = \sqrt{P} \mathbf{w}_0$ with $\|\mathbf{w}_0\|^2 = 1$. Since $\frac{dR_{SK}}{dP} \geq 0$, the optimal P is P_A . Then, consider the function

$$f(x) = \frac{(P_B x + P_A \sigma^2)(x + \sigma^2)}{(P_A \sigma^2 + P_B \sigma^2)x + P_A \sigma^4}, \quad (29)$$

that is monotonically increasing for $x > 0$, since

$$\frac{df(x)}{dx} = \frac{P_B (P_A + P_B)x^2 + 2P_A \sigma^2 x}{\sigma^2 ((P_A + P_B)x + P_A \sigma^2)^2} > 0. \quad (30)$$

Denote $x = \mathbf{w}^T \mathbf{R}_S \mathbf{w}^* (\beta_r \mathbf{v}^H \tilde{\mathbf{R}}_I \mathbf{v} + \beta_{ba})$ and the objective function is $R_{SK} = \log_2 f(x)$. This completes the proof.

APPENDIX C PROOF OF LEMMA 3

Since $\mathbf{w}_{\text{opt}}^T \mathbf{R}_S \mathbf{w}_{\text{opt}}^* = P_A \lambda_{\max}(\mathbf{R}_S)$, we have [9]

$$\lambda_{\max}(\mathbf{R}_S) \approx \lambda_{\max}(\mathbf{R}_h) \lambda_{\max}(\mathbf{R}_v), \quad (31)$$

where $\lambda_{\max}(\cdot)$ returns the maximum eigenvalue of the input matrix. Then, we extend $\mathbf{R}_l, l \in \{h, v\}$ to a circulant matrix

$$\mathbf{R}_l^c = \begin{bmatrix} 1 & \rho & \cdots & \rho^{N_l^t-1} & \rho^{N_l^t-2} & \cdots & \rho^2 & \rho \\ \rho & 1 & \cdots & \rho^{N_l^t-2} & \rho^{N_l^t-1} & \cdots & \rho^3 & \rho^2 \\ \vdots & \vdots & \cdots & \vdots & \vdots & \ddots & \vdots & \vdots \\ \rho & \rho^2 & \cdots & \rho^{N_l^t-2} & \rho^{N_l^t-3} & \cdots & \rho & 1 \end{bmatrix},$$

where $N_l^t \in \{N_H^t, N_V^t\}$ and \mathbf{R}_l is in the first N_l^t rows and N_l^t columns. According to the Cauchy Interlace Theorem [11],

$$\lambda_{\max}(\mathbf{R}_l) \leq \frac{1}{2N_l^t - 1} \mathbf{u}_{\max}^H \mathbf{R}_l^c \mathbf{u}_{\max} = \frac{(1 + \rho)(1 - \rho^{N_l^t-1})}{1 - \rho},$$

where $\mathbf{u}_{\max} = [1, \dots, 1]^T$. Let $\mathbf{x}_0 = \frac{1}{\sqrt{N_l^t}} [1, 1, \dots, 1]^T$ and

$$\lambda_{\max}(\mathbf{R}_l) \geq \mathbf{x}_0^H \mathbf{R}_l \mathbf{x}_0 = \frac{1 + \rho}{1 - \rho} - \frac{2\rho(1 - \rho^{N_l^t})}{N_l^t(1 - \rho)^2}. \quad (32)$$

REFERENCES

- [1] G. Li, C. Sun, W. Xu, M. Di Renzo, and A. Hu, "On maximizing the sum secret key rate for reconfigurable intelligent surface-assisted multiuser systems," *IEEE Trans. Inf. Forensics Security*, vol. 17, pp. 211–225, 2021.
- [2] Z. Ji, P. L. Yeoh, G. Chen, C. Pan, Y. Zhang, Z. He *et al.*, "Random shifting intelligent reflecting surface for OTP encrypted data transmission," *IEEE Wireless Commun. Lett.*, vol. 10, no. 6, pp. 1192–1196, 2021.
- [3] P. Staat, H. Elders-Boll, M. Heinrichs, R. Kronberger, C. Zenger, and C. Paar, "Intelligent reflecting surface-assisted wireless key generation for low-entropy environments," in *Proc. IEEE Int. Symp. Person. Indoor Mobile Radio Commun. (PIMRC)*, Virtual, Sep. 2021, pp. 1–7.
- [4] Z. Ji, P. L. Yeoh, D. Zhang, G. Chen, Y. Zhang, Z. He *et al.*, "Secret key generation for intelligent reflecting surface assisted wireless communication networks," *IEEE Trans. Veh. Technol.*, pp. 1–1, 2020.
- [5] X. Lu, J. Lei, Y. Shi, and W. Li, "Intelligent reflecting surface assisted secret key generation," *IEEE Signal Process. Lett.*, pp. 1–1, 2021.
- [6] E. Björnson and L. Sanguinetti, "Rayleigh fading modeling and channel hardening for reconfigurable intelligent surfaces," *IEEE Wireless Commun. Lett.*, vol. 10, no. 4, pp. 830–834, 2021.
- [7] G. Li, L. Hu, P. Staat, H. Elders-Boll, C. Zenger, C. Paar *et al.*, "Reconfigurable intelligent surface for physical layer key generation: Constructive or destructive?" *accepted by IEEE Wireless Commun.*, 2022.
- [8] D. Neumann, M. Joham, and W. Utschick, "Covariance matrix estimation in massive MIMO," *IEEE Signal Process. Lett.*, vol. 25, no. 6, pp. 863–867, 2018.
- [9] J. Choi and D. J. Love, "Bounds on eigenvalues of a spatial correlation matrix," *IEEE Commun. Lett.*, vol. 18, no. 8, pp. 1391–1394, 2014.
- [10] G. Zhou, C. Pan, H. Ren, K. Wang, and A. Nallanathan, "Outage constrained transmission design for IRS-aided communications with imperfect cascaded channels," in *IEEE Glob. Commun. Conf. (GLOBECOM)*, 2020, pp. 1–6.
- [11] S.-G. Hwang, "Cauchy's interlace theorem for eigenvalues of hermitian matrices," *Am Math Mon.*, vol. 111, no. 2, pp. 157–159, 2004.